Islamic Azad University

Journal of

Optoelectronical Nanostructures

Winter 2024 / Vol. 9, No. 1

Research Paper

A Comparative Study of BSF Layers for InGaN Single-Junction and Multi-Junction Solar Cells

Maryam Amirhoseiny[1] *, Majid Zandi[2], Ahad Kheiri[2]

[1] Department of Engineering Sciences and Physics, Buein Zahra Technical University, Buein Zahra, Qazvin, Iran
[2] Shahid Beheshti University, Tehran, Iran

Received: 11 Oct. 2023
Revised: 17 Nov. 2023
Accepted: 6 Dec. 2023
Published: 15 Mar. 2024

Use your device to scan and read the article online

Keywords:
Back surface field, Heterojunction, InGaN, Simulation, Solar cell

Abstract

The tunability of the InGaN band gap energy over a wide range provides a noble spectral match to sunlight, making it a suitable material for photovoltaic solar cells. The ineffectiveness of single junction solar cell to convert solar full spectrum into electrical energy leads to transparency loss in addition with excess excitation loss. An efficient BSF layer is an essential structural element to attain high efficiency in solar cells. In this work the impact of the BSF layer for InGaN single-junction and multi-junction solar cells is studied using the computational numerical modeling with Silvaco ATLAS simulation technique. The open circuit voltage (Voc) and circuit current density (Jsc) characteristics of the simulated cells and the variation of external quantum efficiency as a function of solar cell structures have been studied. For the optimized cell structure, the maximum Jsc = 14.6 mA/cm^2, Voc = 3.087 V, and fill factor (FF) = 88.15% are obtained under AM1.5G illumination, exhibiting a maximum conversion efficiency of 36.1%.

Citation: Maryam Amirhoseiny, Majid Zandi, Ahad Kheiri. A comparative study of BSF layers for InGaN single-junction and multi-junction solar cells. **Journal of Optoelectronical Nanostructures. 2024; 9 (1): 37- 52.**
DOI: 10.30495/JOPN.2024.31254.1273

***Corresponding author:** Maryam Amirhoseiny
Address: Department of Engineering Sciences and Physics, Buein Zahra Technical University, Buein Zahra, Qazvin, Iran. **Tell:** 00989122044331
Email: Amirhoseiny_m@bzte.ac.ir

INTRODUCTION

The significant appeal of wide band gap nitride-based semiconductors stems from their remarkable capabilities in high power and high frequency device utilization, leading to a recent surge of interest in this field [1,2,3,4]. In materials research, indium gallium nitride (InGaN) has garnered considerable attention due to its distinctive properties among the III-nitride semiconductor family such as high electron and hole mobility, low effective mass, high absorption coefficient, and a great radiation tolerance [5,6,7]. These characteristics lead scientists to use InGaN ternary alloy as a part of high efficiency solar cells.

InGaN is more resistant than materials that are already used in the manufacture of high-efficiency solar cells (like GaAs, InGaP) and can sustain at least twice the radiation that damages those materials, by maintaining its optical and electronic properties [1,8].

Reaching high efficiency solar cells highly depends on the fine tuning of each layer in the solar cell structure [9,10,[11]]. Recombination occurring at the rear section of solar cells plays a critical role in reducing their overall efficiency. This phenomenon arises when charge carriers deviate slightly from the electric field and instead recombine, rather than being collected. To mitigate this issue, a highly doped layer known as the back surface field (BSF) layer is employed. The primary purpose of the BSF layer is to impede this undesired recombination process by redirecting minority carriers back into the cell and attracting majority charge carriers. Thus, an optimized and efficient BSF layer is indispensable for both single junction and multi-junction solar cells [12]. This layer mainly confines the photo-generated minority carriers and retains them to be efficiently collected inside the p-n junction. Researchers have directed their attention towards the potential challenge associated with the utilization of the BSF layer, namely the potential increase in the series resistance of solar cells. So, to improve the device's performance and eliminate design problems modeling and optimization of various layers within a solar cell is so important. However, in order to assess the influence of BSF layers on InGAN solar cells and optimize the structure, we have simulated single-junction and dual-junction $In_xGa_{1-x}N$- based solar cells. The characteristics of open circuit voltage (Voc), short circuit current density (Jsc), and the variation of external quantum efficiency in relation to different solar cell structures have been investigated through simulation.

MODELLING AND SIMULATIONS

Different structures have been simulated in this study; $In_{0.2}Ga_{0.8}N$, $In_{0.4}Ga_{0.6}N$ single junction and , $In_{0.2}Ga_{0.8}N$ / $In_{0.4}Ga_{0.6}N$ double junction solarcells; all with

and without BSF layer. $In_{0.2}Ga_{0.8}N$ / $In_{0.4}Ga_{0.6}N$ dual-junction solar cells structures consist of a top cell, and a bottom cell, which both cells have window layer and BSF. The optimized design is intended to enhance the solar cell's ability to absorb a broader spectrum of incident photons and therefore generate a maximum power output. The schematic of the simulated device and the details of thickness and doping are shown in figure1.

	Contact Gold 0.1 µm			
	Cap n-Type $In_{0.2}Ga_{0.8}N$ 0.3 µm 1e20			
Window	n-Type	$In_{0.2}Ga_{0.8}N$	0.01µm	2.15 e17
Emitter	n-Type	$In_{0.2}Ga_{0.8}N$	0.01µm	1 e16
Base	p-Type	$In_{0.2}Ga_{0.8}N$	X µm	1 e16
	Back Contact			

	Contact Gold 0.1 µm			
	Cap n-Type $In_{0.2}Ga_{0.8}N$ 0.3 µm 1e20			
Window	n-Type	$In_{0.2}Ga_{0.8}N$	0.01µm	2.15 e17
Emitter	n-Type	$In_{0.2}Ga_{0.8}N$	0.01µm	1 e16
Base	p-Type	$In_{0.2}Ga_{0.8}N$	X µm	1 e16
BSF	p-Type	$In_{0.2}Ga_{0.8}N$	0.035 µm	2.15 e19
	Back Contact			

Fig 1: The schematic diagram of the single $In_{0.2}Ga_{0.8}N$ solar cells.

For absorbing maximum solar radiation, a window layer consists of a material with a high band-gap are usually used in solar cell structures [13,14,15]. The selection of materials for the top and bottom cells in a double-junction structure

is based on a progressive increase in band-gap from top to bottom. This arrangement allows the top cell to absorb the shortest wavelengths of solar radiation, while the bottom cell absorbs the longest wavelengths. By efficiently capturing the solar radiation across a wide range of wavelengths, effective absorption of solar energy is achieved [16].

The BSF layer plays a crucial role in the design of a highly efficient solar cell. It serves to confine the photo-generated minority carriers within the cell, ensuring their efficient collection within the p-n junction. Highly doped $In_{0.2}Ga_{0.8}N$ and $In_{0.4}Ga_{0.6}N$ are used as BSF layers in the studied structures.

The solar cell simulation process was carried out using Silvaco ATLAS. The capabilities of this software extend to analyzing the performance of multi-junction solar cells based on III-nitrides, showcasing its potential in this field which has already been reported in some recent works [16,17,18,19]. The Silvaco simulator employs multiple models to compute the cell structure and physical parameters. These include the energy balance transport model, the Concentration-Dependent Low Field Mobility (CONMOB) model, the drift-diffusion transport model, the Optical Recombination (OPTR) model, and the Shockley-Read-Hall (SRH) recombination model. The main parameters utilized to characterize a solar cell include the short circuit current density (JSC), open circuit voltage (VOC), total current (Itotal), field factor (FF), and conversion efficiency (η). These parameters can be determined using the following equations [20,21,22]:

VOC from the ideal diode equation is given by

$$V_{OC} = \frac{nkT}{q} ln\left(\frac{J_{SC}}{J_0} + 1\right), \quad (1)$$

where J0 is the saturation current density, k is the Boltzmann constant, T is the temperature. J0 in equation (5) for each subcell is given by

$$J_0 = qN_C N_V \left[\frac{D_n}{N_A L_n} + \frac{D_p}{N_D L_p}\right] \exp(-\frac{E_g}{kT}), \quad (2)$$

where Di and Li are the diffusion coefficients and the diffusion lengths, respectively, and subscript i denotes either electrons (n) or holes (p). ND and NA are the doping concentrations for donors and acceptors, respectively.

$$J_{total} = J_0 \left[exp\left(\frac{qv}{nkT}\right) - 1\right] - J_{SC}, \quad (3)$$

$$\eta = \frac{V_{OC} I_{SC} FF}{P_{IN}}, \quad (4)$$

$$FF = \frac{V_{OC} - ln(V_{OC} + 0.72)}{V_{OC} + 1}, \quad (5)$$

Here, VOC represents the open-circuit voltage that is normalized to the thermal voltage, denoted as kT/q.

The efficiency of conversion is determined by multiplying the values of VOC, JSC, and FF, and dividing the result by the input power density.

In this study, the characteristics of both single cells, $In_{0.2}Ga_{0.8}N$ and $In_{0.4}Ga_{0.6}N$, are examined both with and without BSF layers. Subsequently, the characteristics of the double junction structure are investigated. Table 1 displays the key parameters for the ternary materials $In_{0.2}Ga_{0.8}N$ and $In_{0.4}Ga_{0.6}N$ employed in this design.

Table 1: Major parameters for the ternary $In_{0.6}$ $Ga_{0.4}N$ and $In_{0.2}$ $Ga_{0.8}N$ materials used in this design

Material	$In_{0.6}Ga_{0.4}N$	$In_{0.2}Ga_{0.8}N$
Band gap Eg (eV) @300 K	1.4448	2.6472
relative permittivity	12.74	10.18
Electronic affinity χ (eV)	7.47	5.15
e mobility (cm^2/VS)	1314.4	1104.8
h mobility (cm^2/VS)	173.9	171.3
State electron density Nc (cm^{-3})	1.46×10^{18}	2.02×10^{18}

State hole density Nv (cm^{-3})	3.9×10^{19}	2.5×10^{19}
Lifetime of electrons and holes Tn_0 and Tp_0 (ns)	1	1

RESULTS AND DISCUSSION

The simulation outcomes of the aforementioned model are illustrated in Figures 2-6. Specifically, Figure 3 displays the J-V curves of four single-junction solar cells comprising In0.2Ga0.8N and In0.4Ga0.6N, both with and without a BSF layer. The observed J-V curve pattern aligns with findings reported in previous studies [[23]24,25, 26]. The outcomes demonstrate that solar cells with In0.2Ga0.8N exhibit superior optical characteristics. The presence of a BSF layer leads to higher Jsc and Voc due to the elevated interface recombination velocity between the layers.

Table 2 presents the values of Jsc, Voc, fill factor, and efficiency for the single-junction solar cells showcased in Figure 3. It can be seen that there is a linear relation between VOC and Eg which is found by substituting the equation (2) into equation (1). Although based on equation (1), VOC is a function of JSC, but after the process of the natural logarithm, VOC varies almost little. In addition, with increasing Eg, JSC decreases with different declining gradients. Typically, photons are absorbed once their energy is higher than the Eg of the material. The declined trend of JSC is intelligible since a rise in Eg makes the practical power density in the spectrum reduced [27, [28]]. The efficiency is calculated from equation (4) as a function of VOC, JSC and FF over the input power density. Consequently, an optimal efficiency can be reached by increasing the VOC and decline the JSC with ascending Eg. The calculated results indicate that single-junction solar cells with $In_{0.2}Ga_{0.8}N$ show higher efficiency than the single-junction solar cells with $In_{0.4}Ga_{0.6}N$ which this observation is consistent with the findings reported in reference [29].

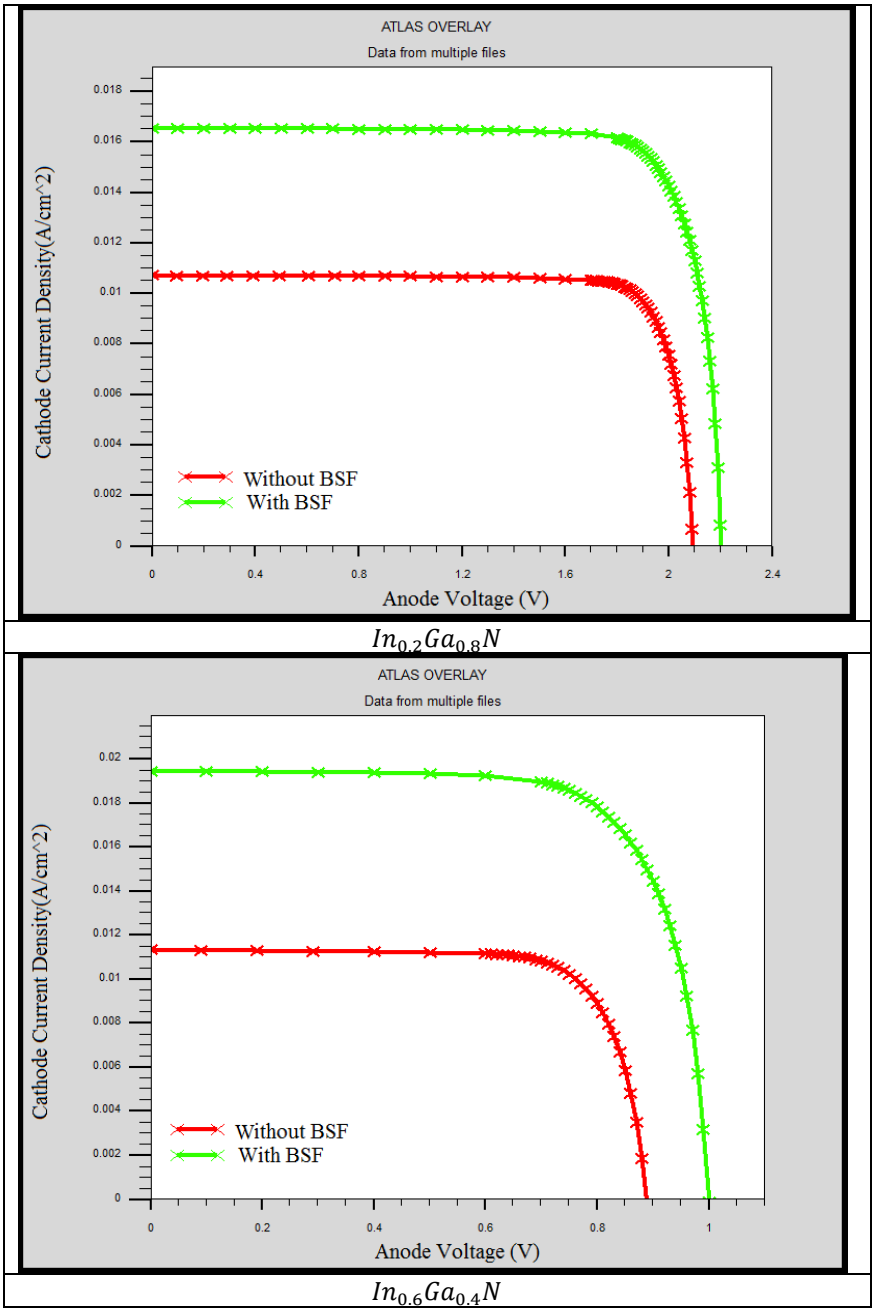

Fig 2: The J-V characteristics curve of cells without and with BSF layers.

The single-junction cell with $In_{0.2}Ga_{0.8}N$ efficiency shown in Table 2 indicates a good prospect. Nevertheless, the simulated InGaN cells can be further optimized by incorporating a BSF window layer, thereby enhancing the achieved efficiency outcomes. It can be seen that the efficiency is significantly increased by adding BSF in both single-junction cells with $In_{0.2}Ga_{0.8}N$ and $In_{0.4}Ga_{0.6}N$.

The inclusion of a BSF layer in the structure resulted in higher values of Voc, Jsc, and FF compared to the cell without a BSF layer. This improvement can be attributed to the reduction in back surface recombination and enhanced formation of the back contact. As a result, the solar cell with a BSF layer exhibited a higher efficiency compared to the cell without one. Specifically, the single-junction cell with In0.2Ga0.8N achieved an efficiency of 26.7%, which is notably higher than the efficiency of 25.1% observed in single-junction Gallium Arsenide cell [**Error! Bookmark not defined.**].

Table2: Jsc, Voc, fill factor, and efficiency of the single-junction solar cells

Structure	$J_{SC}\ (mA/cm^2)$	$V_{OC}(V)$	Fill Factor (FF)	Efficiency (%)
$In_{0.2}Ga_{0.8}N$ cell without BSF	10.72	2.09	83.7	18.7
$In_{0.2}Ga_{0.8}N$ cell with BSF	16.55	2.2	81.5	26.7
$In_{0.6}Ga_{0.4}N$ cell without BSF	11.33	0.88	76.3	7.7
$In_{0.6}Ga_{0.4}N$ cell with BSF	١٩,٤٤	1	73.4	14.2

Figure 3 illustrates a visual depiction of a dual-junction InGaN solar cell. The thicknesses and doping levels of the cell remain consistent with those of the single-junction case involving $In_{0.2}Ga_{0.8}N$ and $In_{0.4}Ga_{0.6}N$. In the dual-junction structure, two layers of single-junction InGaN solar cells are stacked on top of each other. The band gap of the materials decreases progressively from the top to the bottom. This arrangement enables the absorption and conversion of photons with energies greater than the band gap of each respective layer but less than the band gap of the higher layer [30].

		Contact Gold 0.1 µm		
		Cap n-Type $In_{0.2}Ga_{0.8}N$ 0.3 µm 1e20		
Window1	n-Type	$In_{0.2}Ga_{0.8}N$	0.01µm	2.15 e17
Emitter1	n-Type	$In_{0.2}Ga_{0.8}N$	0.01µm	1 e16
Base1	p-Type	$In_{0.2}Ga_{0.8}N$	3.2 µm	1 e16
BSF1	p-Type	$In_{0.2}Ga_{0.8}N$	0.035 µm	2.15 e19
Window2	n-Type	$In_{0.6}Ga_{0.4}N$	0.01µm	2.15 e17
Emitter2	n-Type	$In_{0.6}Ga_{0.4}N$	0.01µm	1 e16
Base2	p-Type	$In_{0.6}Ga_{0.4}N$	3.2 µm	1 e16
BSF2	p-Type	$In_{0.6}Ga_{0.4}N$	0.035 µm	2.15 e19
		Back Contact		

Fig 3: The schematic diagram of the dual-junction solar cells

Figure 4 showcases the J-V curves of the dual-junction solar cell. It is worth noting that, in comparison to Figure 2, the J-V curve for Eg=2.64 eV remained unchanged, whereas the J-V curve for Eg=1.44 eV exhibited a decrease in current. This reduction in current was expected due to the attenuation of the input spectrum by the top cell.

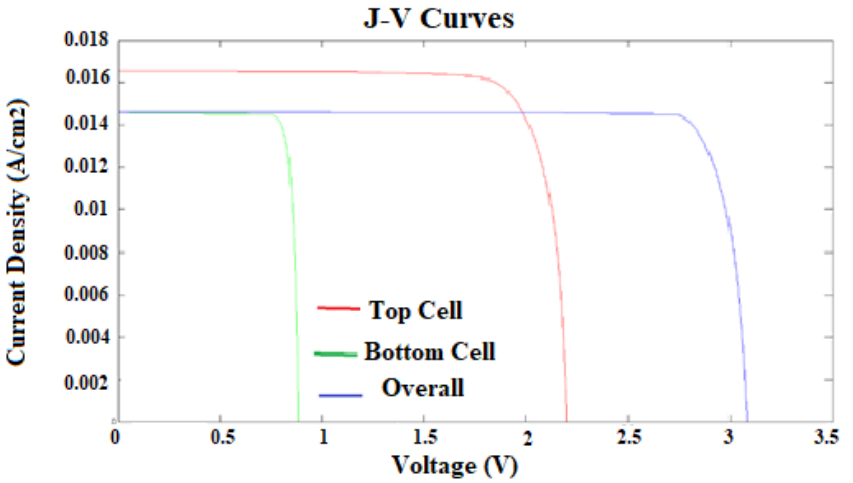

Fig 4: The J-V characteristics curve of cells in double- junction solar cells

Given that the junctions are connected in series, the overall J-V curve is constrained by the J-V curve with the lowest current level. as the same way و the voltages of junctions in series are added. Table 3 presents the efficiency of the dual-junction solar cell, demonstrating a substantial enhancement from the single-junction efficiency (26.7%) to the dual-junction efficiency (36.1%) in InGaN solar cells. This improvement serves as compelling motivation to further advance the development of InGaN solar cells.

Table 3: Jsc, Voc, fill factor, and efficiency of the dual-junction solar cells

Structure	$J_{SC}(mA/cm^2)$	$V_{OC}(V)$	Fill Factor (FF)	Efficiency(%)
$In_{0.2}Ga_{0.8}N$ $/In_{0.6}Ga_{0.4}N$	14.6	3.087	88.15	36.1

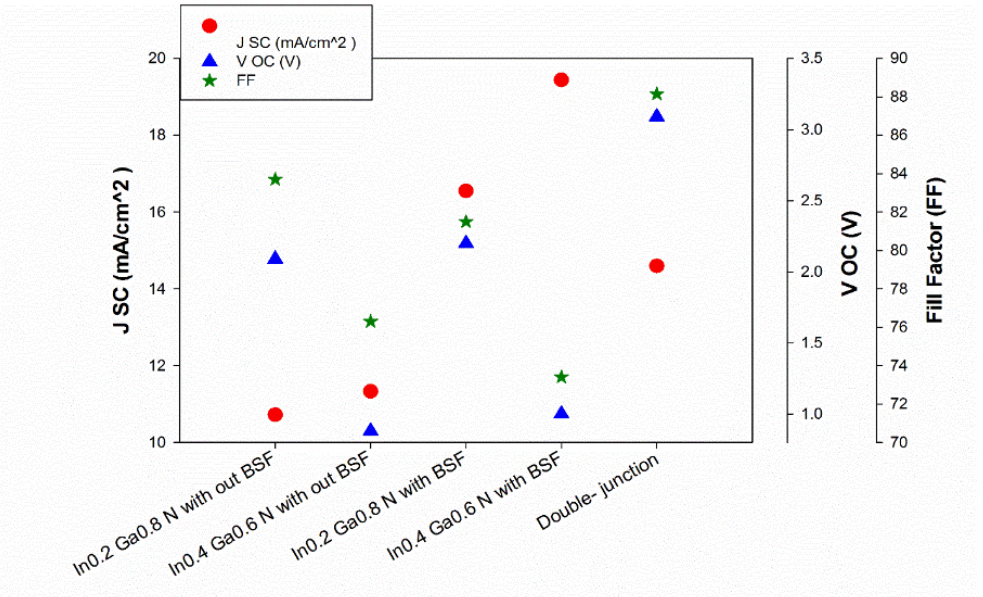

Fig5: Different characteristics of InGaN-based solarcells with different structures

Figure 5 displays the values of Jsc, Voc, fill factor, and efficiency for both single-junction and dual-junction solar cells based on InGaN. Using higher in concentration, decreases the InGaN bandgap and based on equations (1-5), effects on solar cells characteristics. Based on the findings depicted in the figure, it can be observed that as the cell's indium concentration increases, there is a decrease in the open circuit voltage, while the short circuit current density exhibits an increase. Although the inclusion of a BSF layer has led to a slight increase in the open circuit voltage of the single-junction cells, this increment is relatively insignificant. Despite the presence of a minor series resistance introduced by the BSF layer, its impact is overshadowed by the overall positive effect it has on improving the efficiency of the solar cell.

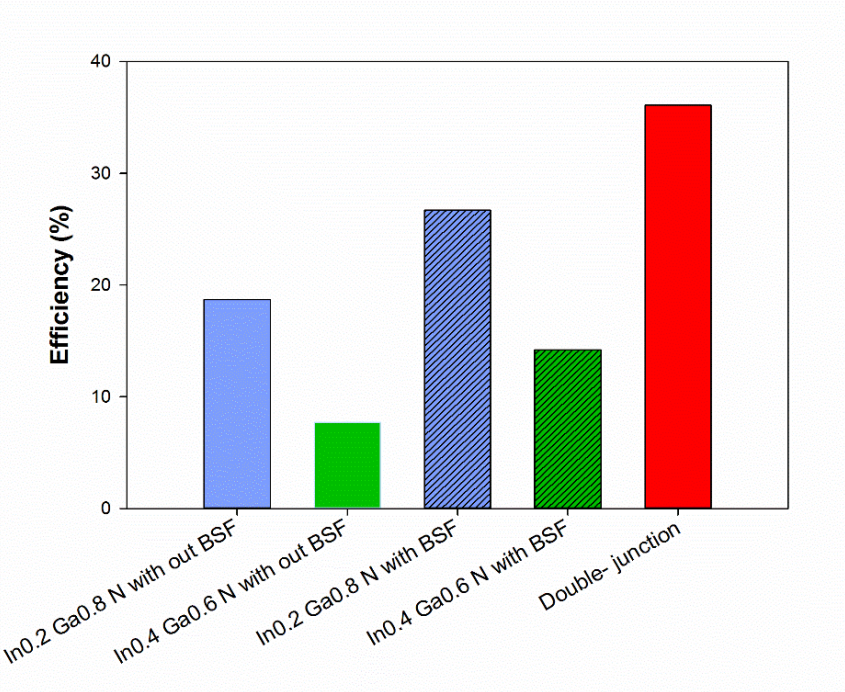

Fig 6: Efficiencies of InGaN-based solar cells with different structures

The efficiency values of InGaN-based solar cells with various structures are depicted in Figure 6. The variations in the efficiency outcomes can be partially ascribed to the disparities in the previously discussed band gap formula. Notably, the inclusion of an effective BSF layer is a critical component in attaining high efficiency in a solar cell. The findings indicate that the efficiency of dual-junction cells surpasses that of single-junction cells. These results align with previous experimental and theoretical studies conducted under similar parameters, thereby corroborating the earlier findings [5, 30]. Any minor deviations can be attributed to variances in the utilized material and optical parameters.

CONCLUSION

This paper presents the simulation results of single and dual-junction Solar Cells characteristics with Silvaco Atlas Software. The results indicate a significant enhancement in the short-circuit current density, open circuit voltage, and efficiency when a BSF layer is incorporated into single-junction cells.

Furthermore, it was observed that dual-junction cells exhibited higher efficiency compared to single-junction cells. This can be attributed to the inherent limitations of single-junction solar cells in efficiently converting the entire solar energy spectrum into electrical energy, leading to losses in transparency and excess excitation. The optimized InGaN cell achieved notable improvements in its performance, with a short-circuit current density (Jsc) of 14.6 mA/cm2, an open circuit voltage (Voc) of 3.087 V, and a remarkable increase in conversion efficiency, reaching up to 36%.

REFERENCES

[1] Alahyarizadeh, G., et al. *Performance of deep violet InGaN double quantum wells laser diodes with quaternary superlattice barriers structure*, Journal of Renewable Energy and Environment. 9(1) (2022) 106-111. Available: https://doi.org/10.30501/jree.2021.300112.1246

[2] Amirhoseiny, M., et al. *Enhancement of deep violet InGaN double quantum wells laser diodes performance characteristics using superlattice last quantum barrier*. Journal of Optoelectronical Nanostructures. 6(2) (2021) 107-120. Available: https://doi.org/10.30495/jopn.2021.4776

[3] Yahyazadeh, Rajab, and Zahra Hashempour. *Non-radiative Auger Current in a InGaN/GaN Multiple Quantum Well Laser Diode under Hydrostatic Pressure and Temperature.* Journal of Optoelectronical Nanostructures 8(2) (2023) 81-107. Available: 10.30495/JOPN.2023.31803.1289

[4] Alahyarizadeh, G and Amirhoseiny, M. *Performance characteristics of deep violet InGaN DQW lasers based on different compliance layers*. Optik, 131 (2017), 194-200. Available: https://doi.org/10.1016/j.ijleo.2016.11.093

[5] Singh, K.J., et al., *Numerical simulation model of compositionally graded optimized radiation hard InGaN multi-junction space solar cell*. Presented at SEISCON 2011. [online]. Available: https://doi.org/10.1049/cp.2011.0453

[6] Alahyarizadeh, G., et al. *Effect of different EBL structures on deep violet InGaN laser diodes performance*. Optics & Laser Technology, 76 (2016) 106-112. Available: https://doi.org/10.1016/j.optlastec.2015.08.007

[7] Alahyarizadeh, G., et al. *Performance enhancement of deep violet InGaN double quantum wells laser diodes with quaternary superlattice barriers*

structure. Journal of Renewable Energy and Environment, 9(1) (2022). 106-111. Available: https://doi.org/10.30501/jree.2021.300112.1246

[8] Amirhoseiny, M., et al. *Effect of annealing temperature on IR-detectors based on InN nanostructures*. Vacuum, 106 (2014). 46-48. Available: https://doi.org/10.1016/j.vacuum.2014.03.010

[9] Al-Ezzi, et al, *Photovoltaic Solar Cells: A Review*. Applied System Innovation. 5(4), (2022) 67. Available: https://doi.org/10.3390/asi5040067

[10] Xu, Tao, and Luping Yu. *How to design low bandgap polymers for highly efficient organic solar cells*. Materials today 17(1) (2014) 11-15. Available: https://doi.org/10.1016/j.mattod.2013.12.005

[11] Yahyazadeh, R., & Hashempour, Z. *Effect of Hydrostatic Pressure on Optical Absorption Coefficient of InGaN/GaN of Multiple Quantum Well Solar Cells.* Journal of Optoelectronical Nanostructures, 6(2) (2021). 1-22. Available: 10.30495/JOPN.2021.27941.1221

[12] Verma, Manish, Soumya R. Routray, and Guru Prasad Mishra. "Analysis and optimization of BSF layer for highly efficient GaInP single junction solar cell." Materials Today: Proceedings 43 (2021) 3420-3423. Available: https://doi.org/10.1016/j.matpr.2020.09.073

[13] Fotis, Konstantinos. *Modeling and simulation of a dual-junction CIGS solar cell using Silvaco ATLAS.* Diss. Monterey, California. Naval Postgraduate School, 2012.

[14] Bouanani, B., et al. Band gap and thickness optimization for improvement of CIGS/CIGS tandem solar cells using Silvaco software. Optik 204 (2020)164217. Available: https://doi.org/10.1016/j.ijleo.2020.164217

[15] Sefidgar, Yagub, Hassan Rasooli Saghai, and Hamed Ghatei Khiabani Azar. "*Enhancing Efficiency of Two-bond Solar Cells Based on GaAs/InGaP*. Journal of Optoelectronical Nanostructures 4(2) (2019) 83-102. Available: 20.1001.1.24237361.2019.4.2.7.7

[16] Galiana, B., et al., *A comparative study of BSF layers for GaAs-based single-junction or multijunction concentrator solar cells*. Semiconductor science and technology. 21(10) (2006)1387. Available: https://doi.org/10.1088/0268-1242/21/10/003

[17] Huang, Xuanqi. *Design and development of high performance III-nitrides photovoltaics.* Diss. Arizona State University, 2020.

[18] Raman, Ashish, Chetan Chaturvedi, and Naveen Kumar. *Multi- Quantum Well- Based Solar Cell*. Electrical and Electronic Devices, Circuits, and Materials: Technological Challenges and Solutions (2021) 351-372. Available: https://doi.org/10.1002/9781119755104.ch19

[19] Madani, Homa Hashemi, Mohammad Reza Shayesteh, and Mohammad Reza. *A Carbon Nanotube (CNT)-based SiGe Thin Film Solar Cell Structure*. Journal of Optoelectronical Nanostructures. 6(1) (2021) 71-86. Available: 10.30495/JOPN.2021.4541

[20] Emery, K., *Photovoltaic efficiency measurements.* In Organic Photovoltaics V. 5520 (2004) 36-44. SPIE. Available: https://doi.org/10.1117/12.562712

[21] Hashemi Nassab, Sayed Mohammad Sadegh, Mohsen Imanieh, and Abbas Kamaly. *The Effect of Doping and the Thickness of the Layers on CIGS Solar Cell Efficiency*. Journal of Optoelectronical Nanostructures 1(1) (2016) 9-24. Available: 20.1001.1.24237361.2016.1.1.2.9

[22] Jacob, N., et al., *Numerical device modeling for direct Z-scheme junctions using a solar cell simulator*. Solar Energy, 259 (2023). 320-327. Available: https://doi.org/10.1016/j.solener.2023.05.013

[23] Häberlin, H. *Photovoltaics: system design and practice*. John Wiley & Sons (2012).

[24] Zhao, Y., et al. *Toward high efficiency at high temperatures: Recent progress and prospects on InGaN-based solar cells.* Materials Today Energy, 31 (2023), 101229. Available: https://doi.org/10.1016/j.mtener.2022.101229

[25] Sarollahi, M., et al., *Study of simulations of double graded InGaN solar cell structures*. Journal of Vacuum Science & Technology B, 40(4) (2022).042203. Available: https://doi.org/10.1116/6.0001841

[26] Shan, H., et al. *Degradation in Efficiency of InGaN/GaN Multiquantum Well Solar Cells With Rising Temperature*. IEEE Transactions on Electron Devices, 69(11) (2022). 6195-6200. Available: https://doi.org/10.1116/6.0001841

[27] Chen, K.-F., C.-L. Hung, and Y.-L. Tsai, *Simulation study of InGaN intermediate-band solar cells*. Journal of Physics D: Applied Physics. 49(48) (2016) 485102. Available: http://dx.doi.org/10.1109/TED.2017.2755069

28 Al-Ezzi, A. S., & Ansari, M. N. M. *Photovoltaic solar cells: a review.* Applied System Innovation, 5(4) (2022), 67. Available: https://doi.org/10.3390/asi5040067

[29] Sabbah, H., *Numerical Simulation of 30% Efficient Lead-Free Perovskite CsSnGeI3-Based Solar Cells*. Materials (Basel). 15(9) (2022) 3229. Available: https://doi.org/10.3390%2Fma15093229

[30] Law, D.C., et al., *Future technology pathways of terrestrial III–V multijunction solar cells for concentrator photovoltaic systems*. Solar Energy Materials and Solar Cells. 94(8) (2010) 1314-1318. Available: https://doi.org/10.1016/j.solmat.2008.07.014